Progress in Biomaterials (2021) 10:173–183
https://doi.org/10.1007/s40204-021-00161-8

ORIGINAL RESEARCH

Magnetic dual-responsive semi-IPN nanogels based on chitosan/PNVCL and study on BSA release behavior

Hamed Mohammad Gholiha[1] · Morteza Ehsani[2,3] · Ardeshir Saeidi[1] · Azam Ghadami[4] · Najmeh Alizadeh[1]

Received: 2 May 2021 / Accepted: 12 July 2021 / Published online: 9 August 2021

Abstract

Magnetic thermoresponsive nanogels present a promising new approach for targeted drug delivery. In the present study, bovine serum albumin (BSA) loaded thermo-responsive magnetic semi-IPN nanogels (MTRSI-NGs) were developed. At first poly(*N*-vinyl caprolactam) (PNVCL) was synthesized by free radical polymerization and then MTRSI-NGs were prepared by crosslinking chitosan in presence of chitosan and Fe_3O_4. The formation of MTRSI-NGs has been confirmed by FTIR, and the average molecular weight of PNVCL was determined by GPC analysis. Rheological and turbidimetry analysis were used to determine lower critical solution temperature (LCST) of PNVCL and magnetic thermo-responsive nanogels (MTRSI-NGs) around 32 and 37 °C, respectively. FE-SEM analysis showed particle size at less than 20 nm in the dried state. Dynamic light scattering determined particle size at about 30 nm in a swelling state. The analysis of release behavior showed that the BSA release ratio at 40 °C was faster than 25 °C. The pH release behavior was evaluated at pH 5.5 and 7.4 and showed that the drug release rate at pH 5.5 was more rapid than pH 7.4. The results show MTRSI-NGs are applicable to protein targeted delivery by thermosensitive targeted drug delivery systems.

Keywords Magnetic thermoresponsive nanogels · Poly(*N*-vinyl caprolactam) · Chitosan nanogel · Albumin release behavior · Target drug delivery · Semi-IPN nanogels

Introduction

Over the last quarter-century, several approaches have been utilized to improve drug efficacy. Different types of drugs such as small molecules, proteins, genes, nucleic acids, etc. are available. Different types of drugs make a great challenge between efficacy and bioavailability. Common drug usages have been encountered with short plasma circulation half-life, susceptibility to rapid degradation in plasma, low aqueous solubility, and high toxicity (Butler et al. 2014). Controlled drug delivery technology has offered many advantages in comparison to conventional drug usage. Smart polymers in drug delivery have excellent potential for improvement of pharmacokinetic properties and increase intracellular uptake of nanocarriers.

Environmental sensitive polymers are one of the most well-known biomaterials which have been applied in drug delivery systems. Macromolecules provide many ways of creating stimuli-sensitive behavior. Smart materials or stimuli-responsive materials can change their behavior by small environmental variations. Stimuli-sensitive polymers can respond to one or more stimuli such as chemical, temperature, light intensity, electric or magnetic pH, field, biological application (Alibolandi et al. 2016; Aguilar et al. 2019; Wang et al. 2014; Ward et al. 2011; Zhuang et al. 2013). Many proteins and drugs are not accessed to specific tissues in sufficient dosages. Drug carriers require precise physicochemical design for targeting such as nanoparticles developed for imaging purposes. Incorporation of magnetic nanoparticles into drugs or protein carriers provide

✉ Morteza Ehsani
M.Ehsani@ippi.ac.ir

Ardeshir Saeidi
ardeshir.saeidi@srbiau.ac.ir

1 Department of Polymer Engineering, Science and Research Branch, Islamic Azad University, Tehran, Iran

2 Department of polymer processing, Iran polymer and petrochemical institute (IPPI), Tehran, Iran

3 Department of Polymer Engineering, Faculty of Engineering,South Tehran Branch, Islamic Azad University, Tehran, Iran

4 Department of Chemical and Polymer Engineering, Central Tehran Branch, Islamic Azad University, Tehran, Iran

advantages, for instance, local protein release, reduction of other tissues drug exposure and minimize side effects, accelerate protein transfer across cell membranes, prevent rapid metabolism or excretion from the body. Magnetic nanocarriers are injected intravenously. The mechanistic action of MTRSI-NGs in the body occurs by three following successions: first, magnetically conducting MTRSI-NGs to targeted tissue, second, the magnet leads to the increasing temperature of Fe_3O_4 and then heat transfer to thermoresponsive nanogels to LCST until to protein release, third wipe out body from MTRSI-NGs (He et al. 2013; Smith et al. 2021; Uhrich et al 1999).Cytotoxicity of PNVCL was investigated by Han et al. The results showed that PNVCL did not show toxicity with short-term cell exposure. PNVCL withstand increases in temperature, while others change from two-phase to single-phase by increasing temperature (Dinari et al. 2021; Fernández-Quiroz et al. 2015; Siirilä et al. 2019; Vihola et al. 2005).Temperature responsive polymers present an excellent hydrophobic-hydrophilic balance in their structure. The slight change in temperature near the cloud point makes the chains collapse. The presence of hydrophilic or hydrophobic polymers in thermo-responsive chains leads to change responding in an aqueous medium and eventually obtain a polymer with new hydrophilic and hydrophilic balances. Most polymers are soluble in water when it is heated, but some water-soluble polymers may collapse from the solution upon heating (Schmidt 2007; Weber et al. 2012). These unique features of thermo-responsive polymers that exhibit biphasic when it's heated above the specific temperature, recognized as a lower critical solution temperature (LCST). The phase transition temperature depends on the hydrogen bonding between water molecules and the functional groups of polymers. Phase or reversible conformational changes take place for thermo-responsive polymers over small variations of temperature. Different types of polymeric materials and systems are known which exhibit thermo-responsive behavior, including hydrogels with a temperature-depending swelling behavior, membranes of thermo-responsive permeability, and materials possessing a change of shape or color upon reaching a certain temperature (Rinaudo 2006). Poly(*N*-vinylcaprolactam) is one of the most popular thermo-responsive polymers that exhibit phase transition temperature around 32 °C. The phase transition temperature can be modified by copolymerization with hydrophobic or hydrophilic polymers (Rao et al 2016). Polysaccharides are well-known hydrophilic biocompatible polymers which are used extensively in drug delivery systems (Yadav and karthikeyan 2019). Among various polysaccharides, chitosan is extensively studied as a nanocarrier of drugs and proteins. Biocompatibility, hydrophilic properties, pH-sensitive, electrostatic force are widely used for target delivery purposes. Phase transition temperature can tune by incorporation of chitosan to PNVCL and crosslinking of chitosan in presence of PNVCL and Fe_3O_4, leads to form thermo-pH responsive magnetic carrier for targeted drug delivery system (Abedini et al. 2018). Banihashemi et al. (2020) investigated the potential of nanocarriers of chitosan-g-PNVCL nanofibers coated with gold–gold sulfide nanoparticles, for controlled release of cisplatin. They found that the higher and faster rate of release was at T > LCST and pH 5.In this study, novel magnetic thermo/pH responsive semi-IPN nanogels were prepared. The phase transition temperature was controlled near human body temperature. Chitosan (CS) was used as an LCST modifier which increases the PNVCL phase transition temperature and it controls the human body. Bovine serum albumin (BSA) was loaded as a model of the protein drug. Two different temperatures were selected to determine drug release behavior at a lower and higher temperature of LCST point. The pH release behavior was reported under two different pH values at 7.4 and 5.5. The novelty of this study is the preparation of thermo-pH dual responsive magnetic nanogels containing hydrophilic protein which exhibits phase transition temperature in the human body, providing new routes for drug delivery systems. Furthermore, it is to investigate the effect of chitosan and magnetic nanoparticles on the phase transition temperature of PNVCL, and evaluate the potential of MTRSI-NGs for use in targeted drug delivery systems as a protein carrier.

Materials and methods

Materials

N-Vinylcaprolactam (NVCL 98%), chitosan medium molecular weight, thioglycolic acid (TG), isopropyl alcohol (IPA), azobisisobutyronitrile (AIBN), sodium tripolyphosphate, 2,2,6,6-tetramethylpiperidin-1-yl)oxyl or (2,2,6,6-tetramethylpiperidin-1-yl)oxidanyl(tempo), $FeCl_2{\cdot}4H_2O$, $FeCl_3{\cdot}6H_2O$, ammonia were purchased from Sigma Aldrich. NaCl, KCl, Na_2HPO_4 $2H_2O$, KH_2PO_4, *N*-hexane supplied from Merck chemical company.

Synthesis of PNVCL

PNVCL was synthesized by controlled free-radical polymerization in IPA solution. First, a mixture of NVCL, TG as a chain transfer agent, and the solvent was added to a sealed flask. The oxygen was removed using a vacuum. Then, AIBN was added to the reaction mixture. The reaction was carried out under a nitrogen atmosphere at 70 °C. After the desired time, the polymerization was stopped and the product was purified by adding anti-solvent *N*-hexane and it was filtered through a Teflon filter under vacuum conditions.

Preparation of magnetite nanoparticles

Iron oxide nanoparticles (Fe_3O_4) were prepared through a controlled chemical co-precipitation method (Kozanoğlu et al. 2011). First, 1 mL of $FeCl_2$ $4H_2O$ 2 M was added into 4 mL of $FeCl_3$ $6H_2O$, 1 M solution (1:2, molar ratio) and mixed for a half hour. Then, 30 mL of 1 M ammonia was incorporated into the mixture under a high-speed mechanical mixer equipped Teflon blade until the precipitate was formed. The precipitated iron oxide was washed three times with deionized water to remove the excess amount of ammonia.

Preparation of magnetic thermo-responsive chitosan poly(N-vinylcaprolactam) semi-IPN nanoparticles (MTRSI-NPs)

Magnetic semi-IPN nanogels were prepared through the suspension cross-linking technique. This method was performed in the 150 mL three-necked flask equipped with a mechanical mixer equipped Teflon blade, condenser, and nitrogen. The poly(*N*-vinylcaprolactam) (PNVCL) was prepared as described previously. An amount of 1 g of PNVCL was dissolved in acetic acid (1% solution) and 0.12 g of chitosan and $Fe_3O_4$was added to a solution. The molar ratio of chitosan and Fe_3O_4 nanoparticles was 1:1 (w/w). Finally, the resulting solution was mixed for 30 min under 1000 rpm and crosslinked by (sodium tripolyphosphate) TPP in a 1:6 (w/w) ratio. The solution was under high-speed mixing at about 1000 rpm until the nanogels formed. The obtained suspension was centrifuged at 4000 rpm for 15 min. To remove the non-reacted component, magnetic nanogels were washed with deionized water several times and centrifuged under previously described conditions. The purified nanogels were dried in a vacuum oven at 30 °C.(see Fig. 1).

Characterization techniques

FTIR spectral studies

Fourier transform infrared (FTIR) measurements were carried to characterize PNVCL polymerization and formation of magnetic chitosan-PNVCL semi-IPN according to the KBr technique using a Bruker-IFS-48 FT-IR spectrometer (Ettlingen, Germany) in the range of 400–5000 cm^{-1}.

Molecular weight analysis

The apparent molecular weights and molecular weight distributions were measured by gel permeation chromatography (GPC) using Agilent-1100 series equipped with a refractive index detector. The solution containing the desired polymer is pumped into a column containing porous particles. GPC is a chromatographic method in which completely dissolved molecules of a polymer are separated by porous columns depending on the size of the molecules. The molecular weight of the test samples is relative and is obtained by comparing its exit time with the calibration curve. This test was performed by a permeable gel chromatography device to determine the average molecular mass of PNVCL polymer samples at 23 °C. First some of the sample was dissolved in tetrahydrofuran as eluent and then in an injection machine with a volume of 20 µL, which was performed at a flow rate of 1 mL/min.

Rheological analysis

Rheology measurements of 10% w/w thermo-responsive suspension/buffer phosphate solutions (pH 7.4) were undertaken using an Anton Paarrheometer with a 50 MM and angle 1 in cone geometry. Solutions were cooled to 5 °C Measurements of complex viscosity (g*), viscous modulus (G″), and elastic modulus (G′) were taken over a range of 5–65 °C and a heating rate of 1 °C/min.

UV–visible spectroscopy

The cloud point of the nanogels as a parameter of LCST determination was analyzed by Shimadzu UV–visible spectrophotometer equipped with a temperature controller. The average of three values was taken as the LCST of nanogels.

Field-emission scanning electron microscopy

To investigate the particle size in dried state FE-SEMMIRA3TESCAN-XMU was utilized. At first, nanogels were dried by freeze-drying technique at − 80 for 24 h, and then nanogels were set on brass equipped with doubled side adhesive and then sputter-coated with gold to enable electric conductivity (Polaron SC515 sputter coater, Fison instruments, Sussex, UK). The measurements were done with an accelerating voltage of 10 kV.

Dynamic light scattering

Dynamic light scattering is a physical technique for measuring particle size in emulsions and suspensions. It is non-destructive and fast to determine the particle size in the range of nm to the micrometer. The measurement was performed with SZ-100 Horbia Join Joyovin in 25 °C and 655 nm.

BSA loading efficacy

Prior to the determination of protein release from the MTRSI-NGs reservoir, loading efficiency was evaluated. The protein encapsulation consists of mixing a certain amount of BSA and MTRSI-NGs (0.2 mg/mL) compound before forming MTRSI-NGs. The protein loading efficiency (LE) and loading capacity (LC) of MTRSI-NGs were evaluated by measuring free BSA unloaded after encapsulation. To measure residual free BSA, the MTRSI-NGs were centrifuged at 4000 rpm for 5 min, and the supernatant was measured using UV–spectrophotometry. The LE and LC were calculated as the following equation (Cheng et al. 2015):

$$\text{LE}\,(\%) = \frac{\text{Total amount of BSA} - \text{Free BSA Total amount of BSA in supernatant}}{\text{Total amount of BSA}} \times 100 \quad (1)$$

$$\text{LC}\,(\%) = \frac{\text{Total amount of BSA} - \text{Free BSA}}{\text{Dried nanoparticle weight}} \times 100 \quad (2)$$

BSA release study

The study of drug release in a temperature-responsive state was performed using a phosphate buffer solution (pH 7.4) at 25 ± 1 and 40 ± 1 °C. BSA loaded MTRSI-NPs nanoparticles (0.2 mg/mL) were added into dialysis bags. Finally, dialysis bags were immersed in 250 mL and the temperatures were set at 25 and 40 °C under mechanical stirrer 50 rpm. The BSA pH release from MTRSI-NPs was measured against PBS (pH7.4 and 5.5) containing at 37 °C. The 3 mL of the medium was withdrawn at the determined time at every 24 h, and 3 mL fresh medium was supplemented. The released amount of BSA was determined using UV–Visible spectroscopy. The release of BSA was expressed as a percentage of the released BSA plotted as a function of time (Zuo et al. 2017).

Results and discussion

FTIR spectral studies

FTIR spectroscopy has been applied to confirm the polymerization of NVCL and other prepared systems. The presence of the amide I band depends on the degree of the hydrogen bonding and the physical state of the compound. FTIR spectra of poly(*N*-vinycaprolactam) and *N*-vinylcaprolactam

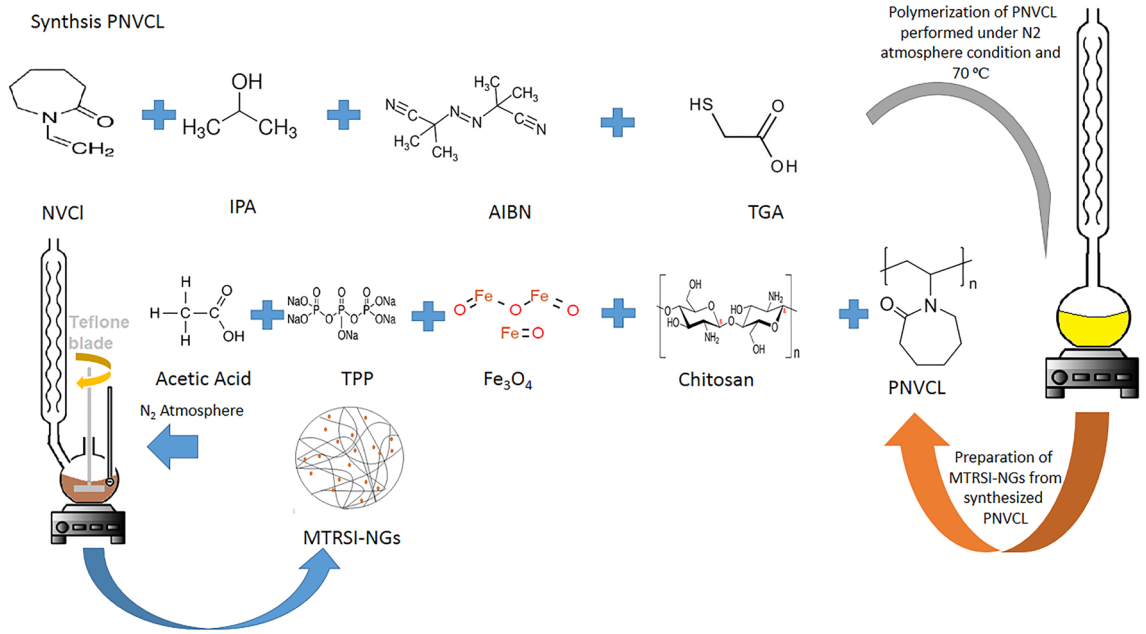

Fig. 1 Scheme of PNVCL synthesis method, and MTRSI-NGs preparation technique

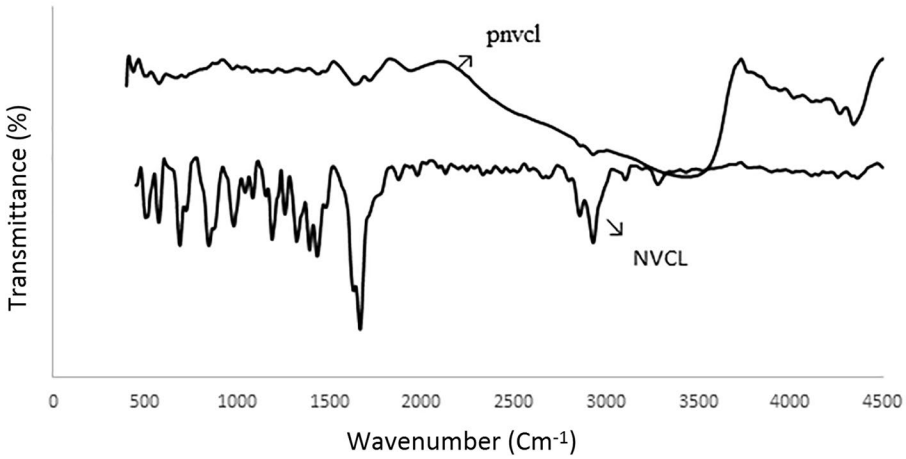

Fig. 2 FTIR spectra of NVCL monomer and PNVCL

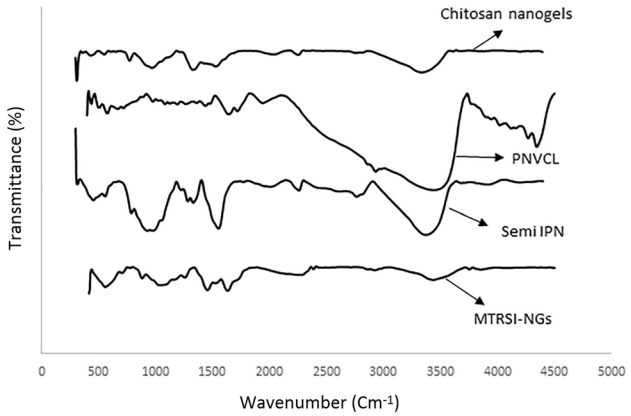

Fig. 3 FTIR spectra of crosslinked chitosan, PNVCL, chitosan PNVCL semi-IPN and MTRSI-NGs

monomer are shown in Fig. 2. The broadband at 3441 cm^{-1} is attributed to the OH stretching of carboxyl groups in the synthesized polymer. The vibration at 2930 and 1433 cm^{-1} assigned to the aliphatic C–H and $–CH_2$ stretching. The dip of 1716 and 1637 cm^{-1} are associated with C = O and amide I band vibrations. The vinyl peaks, (CH and CH_2) in the spectrum of the monomer at 3105 and 981 $cm^{-1}$are disappeared. To confirm the polymerization of NVCL, FTIR spectra of the monomer and the polymer are shown in Fig. 2. It can be concluded from FTIR spectra analysis that the polymer was successfully synthesized and the polymerization proceeds by carbon–carbon double bond opening without any change in the *N*-vinylcaprolactam ring (Kozanoğlu et al. 2011).

Figure 3 demonstrated the FTIR spectra of crosslinked chitosan, PNVCL, chitosan-poly (*N*-vinylcaprolactam)-semi IPN particles, and MTRSI-NGs. The bands in the FTIR spectrum of chitosan can be seen as follows: The amine peak at 1632 in crosslinked chitosan and 1637 in PNVCL were shifted to 1652 cm^{-1} in (PNVCL-CHI)-semi IPN due to the interaction of chitosan with PNVCL. These peaks were attributed to amide I band and carboxylic groups which overlapped with each other (Owens et al. 2007). The semi IPN sample two new peaks appeared. The depth of 1082 was assigned to C–O–C observed in PNVCL and PNVCL-chi semi-IPN samples. Another new peak at 1383 corresponding to CH_2 and OH bending vibrations were due to an interaction of CH_2group presence in PNVCL and OH group in chitosan (Bouillot et al. 2000; Sarkar et al. 2005). The stretching vibration bands at 3443 $cm^{-1}$for chitosan chains and 3441 in PNVCL spectra are shifted to 3470 cm^{-1}thatcorrespond to functional groups of the semi IPN (mainly N–H, O–H). Thus, the results suggested the presence of poly(*N*-vinylcaprolactam) between crosslinked chitosan chains (Patel et al. 2010).

The shift of characteristic peak can explain by two mechanisms:

(1) TPP interaction with the protonated amide and/or amine from the residual chitosan in the semi IPN polymer (Gislén et al 2003),
(2) Interaction of chitosan via PNVCL chain can shift the original position of chitosan and PNVCL.

FTIR spectra of MTRSI-NGs exhibited peaks as can be seen in chitosan and semi-IPN nanogels around 1632 and 1589 cm^{-1} that were attributed to amine and N–H bending vibration of chitosan chains, respectively. The broad bands around 2930, 3440, 1455, and 1054 cm^{-1} were related to the presence of PNVCL chains in MTRSI-NGs. In MTRSI-NGs, a new sharp peak at 560 cm^{-1} appeared that's related to Fe–O groups (Karimzadeh et al. 2017; Zhao et al. 2009). The FTIR spectra demonstrated that chitosan/PNVCL chains were coated on Fe_3O_4 nanoparticles. The negatively surface charged iron oxide has an affinity toward chitosan positively charged chains that could

coat the magnetic nanoparticles by the electrostatic self-assembly oppositely charged and the magnetic semi-IPN nanogels were formed successfully.

Gel permeation chromatography

In order to investigate the molecular weight of poly(N-vinyl-caprolactam) GPC was utilized. The reported GPC data of PNVCL were limited while it has been extensively studied. Molecular weight data from GPC studies illustrate that Mw and Mn were about 3.5 and 2.7 kDa, respectively. The polydispersity index (PDI) was 1.29 calculated from the ratio of Mw/Mn. Although the free radical polymerization has a high conversion rate, the PNVCL conversion rate is low due to NVCL strict hindrance. The phase transition temperature of thermo-responsive polymers is dependent on molecular weight and molecular weight distribution of PNVCL (Lee et al. 2013).

LCST analysis of magnetic nanogels

The phase transition temperature was determined by a UV spectrophotometer-equipped heating system. To determine cloud point temperature, PNVCL and MTRSI-NGs were dispersed in certain concentrations in deionized water. The phase transition temperature for PNVCL was determined about 32 °C while MTRSI-NGs were about 37 °C. In lower temperatures, the solution or suspension is clear while increasing temperature causes clouds to increase in suspension and solution appearance (Namdeo et al. 2008). The increase in phase transition temperature was attributed to changes in the hydrophilic-hydrophobic balance of polymer chains. To confirm turbidimetry results, the rheological analysis in the temperature sweep mode was utilized. The rheological behavior studies are one of the ways to assess the temperature response behavior of these polymers, which is carried out in a wide range of temperatures. Rheological behavior can help explain the LCST processes

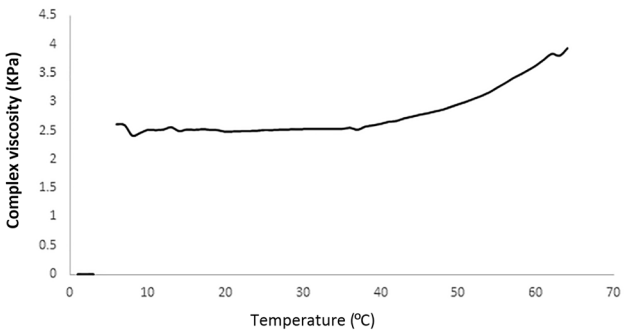

Fig. 4 Rheological analysis of MTRSI-NPs. The viscosity evolves over time during heating to a final temperature

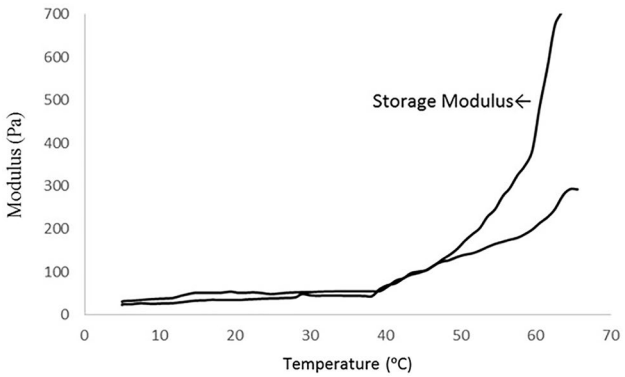

Fig. 5 Rheological analysis of MTRSI-NPs. Variation storage and loss modulus against temperature

in nanoparticles with their performance in response to shear rates applied by changing temperatures. Figures 4 and 5 show the results of rheological test in a temperature state. Figure 4 exhibited chitosan nanoparticles' rheological behavior that showed the decrease in complex viscosity, storage, and loss modulus by increasing temperature, while it demonstrated an increase in complex viscosity, storage modulus, and loss modulus for magnetic semi IPN nanogels. MTRSI-NGs curve demonstrates that when temperature rises to higher than LCST, the value of viscosity and modulus curve rises (Huang et al. 2017; Smith et al. 2021). As shown in Figs. 4 and 5, a significant increase in complex viscosity, storage modules, and the loss modulus are observed by increasing temperature. The modulus of elasticity shows the amount of energy storage and its recovery in each cycle of behavioral change. Therefore, the modulus of elasticity is low at temperatures below the LCST temperature and increases with increasing temperature up to the temperature of LCST. Rheometry results confirmed FTIR results for preparation thermo-responsive nanogels by exhibition increasing in modulus and complex viscosity for magnetic semi-IPN nanogels. On the one hand increasing in complex viscosity and modulus have occurred at 38 °C that is confirmed by turbidimetry results. Phase transition temperature has been evaluated in the human body temperature range that can provide a suitable carrier for target protein delivery. In most polymers, the elastic modulus and complex viscosity decrease by increasing temperature, in contrast to other polymers in temperature-responsive polymers that are attributed to chain conformation. This phenomenon can be explained by the disappearance of hydrogen interactions between thermo-responsive polymer nanoparticles and water molecules that caused conformation changes from a random coil to a globule (Cheng et al. 2013). In the case of suspensions, the phase transition temperature is explained by their collapse. It means when the temperature is below the LCST, the particles are stable and are completely dispersed

due to strong hydrogen bonding between poly(*N*-vinylcaprolactam) chains and environmental aqueous. Increasing temperature in thermo-responsive suspension causes the collapse of the nanogels due to dissipated hydrogen bonding between thermo-responsive nanogels and environmental aqueous change in chain conformation leading to an increase in modulus. As seen in Fig. 5 thermo-responsive nanogels exhibited higher loss modulus in comparison with storage modulus at lower LCST temperature, while storage modulus was higher than loss modulus at the upper phase transition temperature. The differences in storage and loss modulus are due to the change in the conformation of thermo-responsive polymer chains at above LCST. In a monophasic state the PNVCL chains conformation is random coil that causes it to display a higher loss modulus, while in the biphasic state, the chains transform to a globule. Globule conformation can provide storage energy more than a random coil. By increasing temperature up to LCST, storage modulus and loss modulus significantly increased that illustrated phase transition temperature. Thermo-responsive nanogels behave like a hard-sphere which loss modulus is higher than storage modulus in lower temperature (G′ > G″). By increasing temperature up to phase transition temperature, suspension behavior was changed, and storage modulus became almost equal to loss modulus.

Particles size analysis

Particle size analysis was evaluated in dried and swelled condition. FE-SEM analysis was applied to investigate chitosan and magnetic semi-IPN nanogels in the dehydrated state. Figure 6 exhibits FE-SEM analysis of dehydrated pure chitosan and semi-IPN magnetic nanogels. By changing different parameters in preparation methods such as stirring speed, reaction temperature, sample pH can control nanogels size. FE-SEM images indicated that dehydrated chitosan nanogels size in the range of 30–40 nm was non-uniform. The size of MTRSI particles was about 20 nm. The reason for decreasing particle size in MTRSI particles is attributed to the presence of magnetic nanoparticles. The presence of magnetic nanoparticles caused to increase ionization degree that leads to reduced particle size. The ionization degree that depends on pH value is the most critical parameter that determines particle size during hybrid nanogels forming (Sahu et al. 2011). MTRSI nanogels morphology is more spherical than chitosan. One reason for controlling the shape and structure of nano gels is the presence of chain caprolactam in the MTRSI nanogels, which prevents nanoparticle deformation and strengthens the nanoparticles in the dehydrated state. Preserving the spherical form of nanoparticles in pharmacological systems is the critical parameter (Sadighian et al. 2015).

To investigate the size of nanogels in a swelling state, dynamic light scattering was utilized. DLS exhibited particles size around 30 nm and almost mono dispersed which was appropriate for local drug delivery. The present results can be obtained by the presence of acetic acid in preparation MTRSI-NGs that causes high dispersion of magnetic nanoparticles and decrease particles size while it was formed. The most important factor for decreasing particle size is attributed to the presence of PNVCL chains in chitosan nanoparticle cavities, which reduced free volume. High-speed mixing is another substantial parameter caused by polymer and iron oxide dispersed well and its formation in the smaller size. The difference between particle size of FE-SEM and DLS measurement can be related to measurement conditions. The DLS evaluated the hydrodynamic particles size while FE-SEM was analyzed in a dried mood (Elzoghby et al. 2012).(see Fig. 7).

Drug release behavior

MTRSI-NGs loaded bovine serum albumin drug release behavior was evaluated under different temperatures at pH. The BSA was used as a type of protein for studying the controlled release of proteins from nanogels which were widely used (Tong et al. 1996). The various physical and chemical parameters affect drug release behavior such as temperature, pH, the molecular weight of polymer and drug, preparation condition of nanogels, drug concentration.

To investigate, the effect of temperature on drug release behavior two different temperatures were selected. The drug release test was carried out at 25 ± 1 and 40 ± 1 °C and in constant pH at 7.4. As shown in Fig. 8 bovine serum albumin release ratio at 40 °C was faster in comparison with 25 °C which indicates the importance of phase transition temperature. The BSA release behavior at 40 °C suggests that more than 70% of the protein in MTRSI-NPs sample was released from the nanoparticles in 3 first days when the drug release rate at 25 °C was slower than 40 °C. The higher release ratio was at the first three days of the test, which was attributed to BSA release from the vicinity of the surface of nanoparticles. By comparing drug release at 25 and 40 °C, the LCST effect is understandable. The release behavior at a higher temperature of LCST is faster than at the lower temperature of LCST. The main reason for describing this behavior changes in hydrophilic properties at the higher temperature of LCST which caused a change in nature of the hydrophilic to hydrophobic (Ta and Pulat et al. 2012).

Drug release kinetics evaluated in pH 7.4 and 5.5. The release behavior indicates that pH strongly influenced bovine serum albumin release through MTRSI-NGs. As shown in Fig. 9, more than 50% of BSA was released after 3 days at pH 5.5, while this amount was about 30%at pH 7.4. This behavior is explained by shrinking MTRSI-NGs

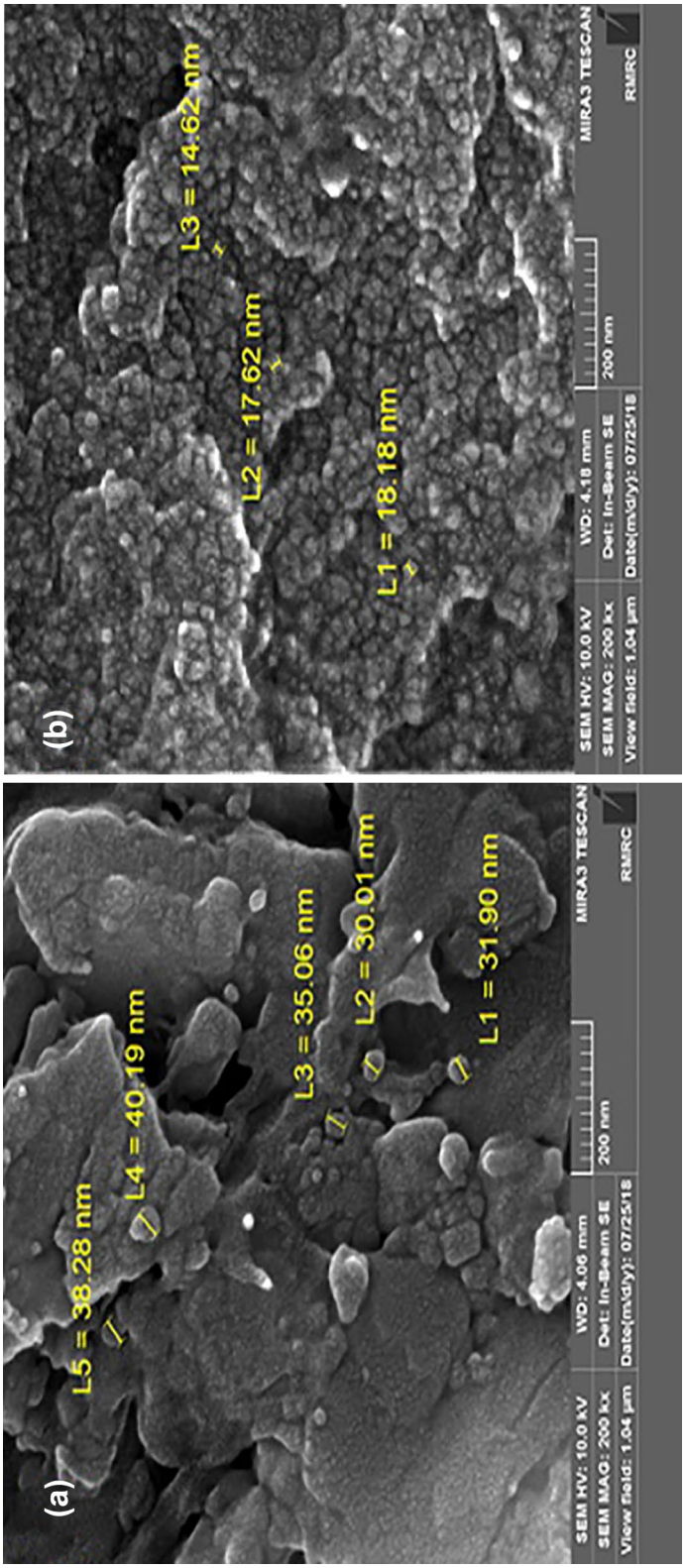

Fig. 6 FESEM images of **a** Chitosan nanogels, **b** MTRSI-NGs

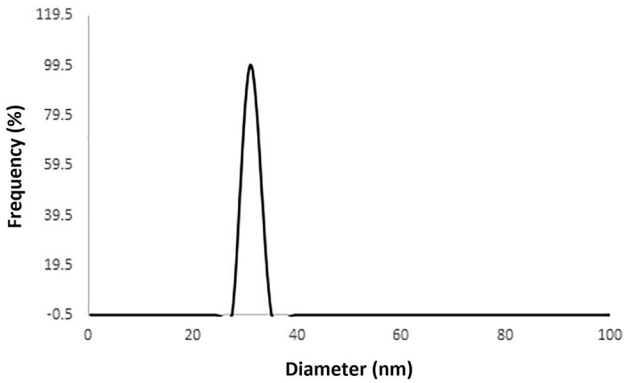

Fig. 7 Dynamic light scattering analysis of MTRSI nanogels

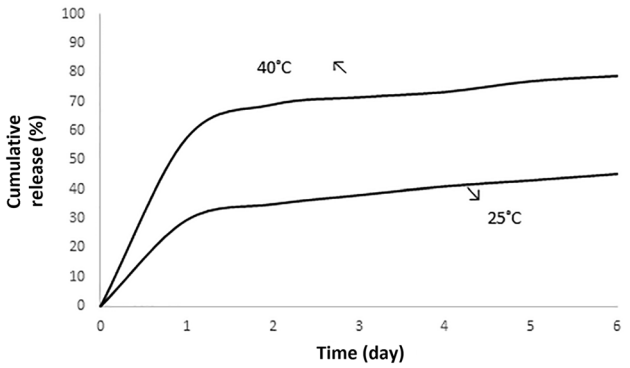

Fig. 8 In vitro release profiles of BSA from MTRSI-NGs in PBS solution (Temperature 25 and 40 °C)

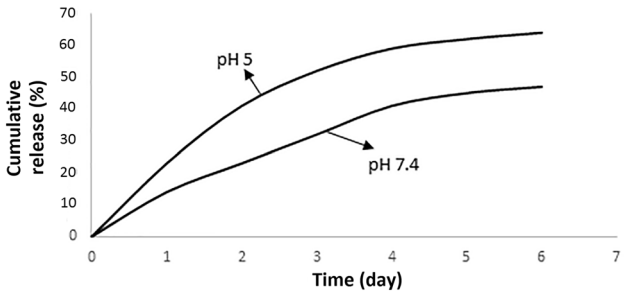

Fig. 9 In vitro release profiles of BSA from MTRSI-NGs in PBS solution (pH 5.5, 7.4)

in pH 7.4 that prevents albumin release through the nanogels. A fast release profile for pH 5.5 is attributed to the swelling behavior of nanogels due to the pH-responsive properties of MTRSI-NGs. The BSA release behaviors represented unstable behavior nanogels under different pH values and temperatures. According to MTRSI-NGs results, they only prevented the high ratio release of proteins in pH 7.4 and temperature at 25 °C. The obtained results illustrated that protein-carrying nanoparticles are suitable for use in protein delivery to internal organs and tissues due to the long release time of the protein (Ta and Pulat et al. 2012).

Conclusion

In the present study, magnetic thermo-responsive semi-IPN nanogels are optimized for the local protein delivery systems. At first, PNVCL was synthesized through free radical polymerization and the MTRSI-NGs were prepared. FTIR spectra demonstrate that magnetic semi-IPN nanogels were formed successfully. Gel permeation chromatography exhibited a low molecular weight of PNVCL synthesis. Thermo-responsive properties of MTRSI-NGs were analyzed by turbidimetry and rheometry. Turbidimetry exhibits cloud point around 37 °C. The results of turbidimetry were confirmed by rheological analysis in temperature sweep mood. Phase transition results demonstrated that MTRSI-NGs are controlled near human body temperature. To study particle size in the dried and swelling mood, FE-SEM and dynamic light scattering were utilized. FE-SEM analysis displayed particle sizes less than 20 nm while pure chitosan was between 30 and 40 nm due to high ionization properties of magnetic nanoparticles present in MTRSI-NGs structure. Dynamic light scattering analysis showed nanogels size about 30 nm in swelling mood. The determination of protein release treatment of MTRSI-NGs showed a higher ratio of drug release at 40 in comparison with 25 °C that is attributed to the switching hydrophobicity properties of MTRSI-NGs after phase transition temperature. Furthermore, drug release behavior of MTRSI-NGs is given at different pH values. The release behavior at pH 5.5 showed a higher ratio in comparison with 7.4 that indicates the pH-sensitive properties of MTRSI-NGs. The present study suggests that chitosan leads to modifying the LCST behavior of PNVCL to the near-human body. These results indicate that MTRSI-NGs are appropriate for the target protein delivery system.

Acknowledgements This research was supported by the Science and Research branch of Islamic Azad University and also Iran polymer and petrochemical institute.

Declarations

Conflict of interest The authors declare no conflict of interest.

Ethical approval This article does not contain any studies with human participants or animals performed by any of the authors.

References

Abedini F, Ebrahimi M, Roozbehani AH, Domb AJ, Hosseinkhani H (2018) Overview on natural hydrophilic polysaccharide polymers in drug delivery. Polym Adv Tech 29(10):2564–2573. https://doi.org/10.1002/pat.4375

Aguilar MR, San Román J (2019) Introduction to smart polymers and their applications. In: Aguilar MR, San Román J (eds) Smart polymers and their applications. Woodhead Publishing, Cambridge, pp 1–11

Alibolandi M, Abnous K, Sadeghi F, Hosseinkhani H, Ramezani M, Hadizadeh F (2016) Folate receptor-targeted multimodal polymersomes for delivery of quantum dots and doxorubicin to breast adenocarcinoma: in vitro and in vivo evaluation. Int J Pharm 500(1–2):162–178. https://doi.org/10.1016/j.ijpharm.2016.01.040

Banihashem S, Nezhati MN, Panahia HA (2020) Synthesis of chitosan-grafted-poly (*N*-vinylcaprolactam) coated on the thiolated gold nanoparticles surface for controlled release of cisplatin. Carboh Polym 227:115333. https://doi.org/10.1016/j.carbpol.2019.115333

Bouillot P, Vincent B (2000) A comparison of the swelling behaviour of copolymer and interpenetrating network microgel particles. Colloid Polym Sci 278(1):74–79. https://doi.org/10.1007/s003960050012

Butler IS, Gilson DF (2014) A theoretical investigation of the products in the Frankland reaction of dimethylzinc compounds with nitric oxide. Can J Chem 92(10):948–950. https://doi.org/10.1139/cjc-2014-0049

Cheng R, Meng F, Deng C, Klok HA, Zhong Z (2013) Dual and multi-stimuli responsive polymeric nanoparticles for programmed site-specific drug delivery. Biomaterials 34(14):3647–3657. https://doi.org/10.1016/j.biomaterials.2013.01.084

Cheng L, Bulmer C, Margaritis A (2015) Characterization of novel composite alginate chitosan–carrageenan nanoparticles for encapsulation of BSA as a model drug delivery system. Curr Drug Deliv 12(3):351–357

Dinari A, Abdollahi M, Sadeghizadeh M (2021) Design and fabrication of dual responsive lignin- based nanogel via "grafting from" atom transfer radical polymerization for curcumin loading and release. Sci Rep 11(1):1–16. https://doi.org/10.1038/s41598-021-81393-3

Elzoghby AO, Samy WM, Elgindy NA (2012) Albumin-based nanoparticles as potential controlled release drug delivery systems. J Control Release 157(2):168–182. https://doi.org/10.1016/j.jconrel.2011.07.031

Fernández-Quiroz D, González-Gómez Á, Lizardi-Mendoza J, Vázquez-Lasa B, Goycoolea FM, San Román J, Argüelles-Monal WM (2015) Effect of the molecular architecture on the thermosensitive properties of chitosan-g-poly (*N*-vinylcaprolactam). Carbohyd Polym 134:92–101. https://doi.org/10.1016/j.carbpol.2015.07.069

Gislén A, Dacke M, Kröger RH, Abrahamsson M, Nilsson DE, Warrant EJ (2003) Superior underwater vision in a human population of sea gypsies. Curr Biol 13(10):833–836. https://doi.org/10.1016/S0960-9822(03)00290-2

He WJ, Hosseinkhani H, Hong PD, Chiang CH, Yu DS (2013) Magnetic nanoparticles for imaging technology. Int J Nanotech 10(10–11):930–944. https://doi.org/10.1504/IJNT.2013.058120

Huang Y, Yong P, Chen Y, Gao Y, Xu W, Lv Y, Yang L, Reis RL, Pirraco RP, Chen J (2017) Micellization and gelatinization in aqueous media of pH-and thermo-responsive amphiphilic ABC (PMMA 82-b-PDMAEMA 150-b-PNIPAM 65) triblock copolymer synthesized by consecutive RAFT polymerization. RSC Adv 7(46):28711–28722. https://doi.org/10.1039/C7RA04351A

Karimzadeh I, Aghazadeh M, Doroudi T, Reza Ganjali M, Hossein Kolivand P (2017) Effective preparation, characterization and in situ surface coating of super paramagnetic Fe_3O_4 nanoparticles with polyethyleneimine through cathodic electrochemical deposition (CED). Curr Nano Sci 13(2):167–174

Kozanoğlu S, Özdemir T, Usanmaz A (2011) Polymerization of *N*-vinylcaprolactam and characterization of poly (*N*-vinylcaprolactam). J Macromol Sci Part A 48(6):467–477. https://doi.org/10.1080/10601325.2011.573350

Lee B, Jiao A, Yu S, You JB, Kim DH, Im SG (2013) Initiated chemical vapor deposition of thermoresponsive poly (*N*-vinylcaprolactam) thin films for cell sheet engineering. Acta Biomater 9(8):7691–7698. https://doi.org/10.1016/j.actbio.2013.04.049

Namdeo M, Saxena S, Tankhiwale R, Bajpai M, Mohan YÁ, Bajpai SK (2008) Magnetic nanoparticles for drug delivery applications. J Nanosci Nanotech 8(7):3247–3271. https://doi.org/10.1166/jnn.2008.399

Owens DE, Jian Y, Fang JE, Slaughter BV, Chen YH, Peppas NA (2007) Thermally responsive swelling properties of polyacrylamide/poly (acrylic acid) interpenetrating polymer network nanoparticles. Macromolecules 40(20):7306–7310. https://doi.org/10.1021/ma071089x

Patel MP, Patel RR, Patel JK (2010) Chitosan mediated targeted drug delivery system: a review. J Pharm Pharm Sci 13(4):536–557. https://doi.org/10.18433/J3JC7C

Rao KM, Rao K, Ha CS (2016) Stimuli responsive poly (*N*-vinylcaprolactam) gels for biomedical applications. Gels 2(1):6. https://doi.org/10.3390/gels2010006

Rinaudo M (2006) Chitin and chitosan: properties and applications. Prog Polym Sci 31(7):603–632. https://doi.org/10.1016/j.progpolymsci.2006.06.001

Sadighian S, Hosseini-Monfared H, Rostamizadeh K, Hamidi M (2015) pH-Triggered magnetic-chitosan nanogels (MCNs) for doxorubicin delivery: physically vs. chemically cross-linking approach. Adv Pharm Bullet 5(1):115. https://doi.org/10.5681/apb.2015.016

Sahu SK, Maiti S, Maiti TK, Ghosh SK, Pramanik P (2011) Hydrophobically modified carboxymethyl chitosan nanoparticles targeted delivery of paclitaxel. J Drug Target 19(2):104–113. https://doi.org/10.3109/10611861003733987

Sarkar D, El-Khoury J, Lopina ST, Hu J (2005) An effective method for preparing polymer nanocapsules with hydrophobic acrylic shell and hydrophilic interior by inverse emulsion radical polymerization. Macromolecules 38(20):8603–8605. https://doi.org/10.1021/ma050661m

Schmidt AM (2007) Thermoresponsive magnetic colloids. Colloid Polym Sci 285(9):953–966. https://doi.org/10.1007/s00396-007-1667-z

Siirilä J, Karesoja M, Pulkkinen P, Malho JM, Tenhu H (2019) Soft poly (*N*- vinylcaprolactam) nanogels surface-decorated with AuNPs. Response to temperature, light, and RF-field. Euro Polym J 115:59–69. https://doi.org/10.1016/j.eurpolymj.2019.03.010

Smith AA, Maikawa CL, Hernandez HL, Appel EA (2021) Controlling properties of thermogels by tuning critical solution behaviour of ternary copolymers. Polym Chem 12(13):1918–1923. https://doi.org/10.1039/D0PY01696A

Ta RS, Pulat M (2012) 5-fluorouracil encapsulated chitosan nanoparticles for pH-stimulated drug delivery: evaluation of controlled release kinetics. J Nanomater. https://doi.org/10.1155/2012/313961

Tong J, Anderson JL (1996) Partitioning and diffusion of proteins and linear polymers in polyacrylamide gels. Biophys J 70(3):1505–1513. https://doi.org/10.1016/S0006-3495(96)79712-6

Uhrich KE, Cannizzaro SM, Langer RS, Shakesheff KM (1999) Polymeric systems for controlled drug release. Chem Rev Colum 99(11):3181–3198

Vihola H, Laukkanen A, Valtola L, Tenhu H, Hirvonen J (2005) Cytotoxicity of thermosensitive polymers poly (*N*-isopropylacrylamide), poly (*N*-vinylcaprolactam) and amphiphilically modified

poly (*N*-vinylcaprolactam). Biomaterials 26(16):3055–3064. https://doi.org/10.1016/j.biomaterials.2004.09.008

Wang Y, Shim MS, Levinson NS, Sung HW, Xia Y (2014) Stimuli-responsive materials for controlled release of theranostic agents. Adv Funct Mater 24(27):4206–4220. https://doi.org/10.1002/adfm.201400279

Ward MA, Georgiou TK (2011) Thermoresponsive polymers for biomedical applications. Polymers 3(3):1215–1242. https://doi.org/10.3390/polym3031215

Weber C, Hoogenboom R, Schubert US (2012) Temperature responsive bio-compatible polymers based on poly (ethylene oxide) and poly (2-oxazoline) s. Prog Polym Sci 37(5):686–714. https://doi.org/10.1016/j.progpolymsci.2011.10.002

Yadav H, Karthikeyan C (2019) Natural polysaccharides: structural features and properties. In: Yadav H (ed) Polysaccharide carriers for drug delivery. Woodhead Publishing, Cambridge, pp 1–17

Zhao DL, Wang XX, Zeng XW, Xia QS, Tang JT (2009) Preparation and inductive heating property of Fe_3O_4–chitosan composite nanoparticles in an AC magnetic field for localized hyperthermia. J Alloy Compd 477(1–2):739–743. https://doi.org/10.1016/j.jallcom.2008.10.104

Zhuang J, Gordon MR, Ventura J, Li L, Thayumanavan S (2013) Multi-stimuli responsive macromolecules and their assemblies. Chem Soc Rev 42(17):7421–7435. https://doi.org/10.1039/C3CS60094G

Zuo Y, Kong M, Mu Y, Feng C, Chen X (2017) Chitosan based nanogels stepwise response to intracellular delivery kinetics for enhanced delivery of doxorubicin. Int J Biol Macromol 104:157–164. https://doi.org/10.1016/j.ijbiomac.2017.06.020